Journal of Dental Sciences 19 (2024) 1680–1690

Available online at www.sciencedirect.com

ScienceDirect

journal homepage: www.e-jds.com

The histone deacetylase inhibitor MS-275 enhances the matrix mineralization of dental pulp stem cells by inducing fibronectin expression

Shigeki Suzuki*, Kento Sasaki, Rahmad Rifqi Fahreza, Eiji Nemoto, Satoru Yamada

Department of Periodontology and Endodontology, Tohoku University Graduate School of Dentistry, Sendai, Japan

Received 6 November 2023; Final revision received 24 November 2023
Available online 3 December 2023

KEYWORDS
Odontogenic differentiation;
Histone deacetylase (HDACs) inhibitor;
MS-275;
ATACseq;
RNA-seq;
Fibronectin

Abstract *Background/purpose:* The acetylation of histone H3 proteins keeps local chromatin regions open and accessible, thereby facilitating transcriptional events. We recently reported integrative epigenomic and transcriptome analyses of differentiating dental pulp stem cells (DPSCs). A significant increase in the number of super-enhancers, which are local genomic locations marked by condensed open chromatin peaks that facilitate transcriptional events, in differentiating DPSCs were observed. However, it is still unclear whether histone deacetylase (HDACs) inhibitors (HDACis) have beneficial effects on the odontogenic differentiation of DPSCs and on the matrix mineralization-inducing ability of DPSCs.

Materials and methods: DPSCs were cultured in an odontogenic induction medium for a prolonged period in the presence of HDACis, MS-275 and Trichostatin A (TSA). ATAC-seq and RNA-seq samples were collected from differentiating DPSCs to explore the epigenomic and transcriptomic alterations induced by HDACis and identify key target proteins that mediate HDACis-induced phenotypic changes.

Results: MS-275 and TSA did not change whole-genome open chromatin accessibility or increase odontogenic differentiation, as assessed by alkaline phosphate activity. However, the matrix mineralization-inducing ability assessed by calcified nodule formation was significantly increased by MS-275 but not by TSA. FN1, which encodes fibronectin, was identified as upregulated by MS-275. The knockdown of fibronectin evidently suppressed MS-275-induced calcified nodule formation.

Conclusion: MS-275 induced calcified nodule formation by the mechanistic upregulation of FN1, independent of epigenomic alterations. Hence, the application of MS-275 as direct

* Corresponding author. Department of Periodontology and Endodontology, Tohoku University Graduate School of Dentistry; 4-1, Seiryo-machi, Aoba-ku, Sendai, 980-8575, Japan.
E-mail address: shigeki.suzuki.b1@tohoku.ac.jp (S. Suzuki).

https://doi.org/10.1016/j.jds.2023.11.019

capping materials has therapeutic potential for promoting reparative dentin formation by constructing a fibronectin-organizing physiological extracellular matrix environment that is adequate for matrix mineralization.

Introduction

Histone acetylation in nucleosomes, both at the gene locus and within the distal and mesial enhancer regions, has been linked to active gene transcription. The degree of acetylation is regulated by histone acetyltransferase, which catalyzes the transfer of an acetyl group from acetyl-CoA to lysine residues, and by histone deacetylase (HDAC), which promotes the removal of the acetyl group from lysine residues.[1—3] Thus, HDAC inhibitors (HDACis) increase chromatin accessibility, thereby accelerating subsequent transcriptional events. HDACis also maintain the acetylation status of various non-histone substrates; thus, the effects of HDACis are not always believed to arise from histone-mediated epigenomic alterations.[4]

Dental pulp stem cells (DPSCs), isolated from permanent teeth using general mesenchymal stem cell markers, have multi-regenerative abilities and are widely recognized for their roles in inducing dentin and pulp regeneration and in maintaining dental pulp tissue homeostasis through their odontogenic differentiation and immunomodulatory abilities.[5—8] Changes in histone acetylation and deacetylation in specific gene loci during the odontogenic differentiation of DPSCs have been revealed.[9] p300 is a transcriptional co-activator with histone acetyltransferase activity. Suppression of p300 inhibited the odontogenic abilities of DPSCs, which were estimated by alkaline phosphatase activity, calcified nodule formation, and the *dentin matrix protein-1* (*DMP-1*) and *dentin sialophosphoprotein* (*DSPP*) expression levels, known markers of odontogenic differentiation.[10—12] p300 facilitated the acetylation of lysine 9 of histone H3 in the promoter regions of *Osteocalcin* and *DSPP* to induce odontogenic differentiation.[13] Krüppel-like factor 4 (KLF4), a key transcription factor for terminal odontogenic differentiation, is associated with p300 to transactivate *Dmp1* and *Osterix*,[14] Recently, an inhibitor of nuclear factor kappa Bζ (IκBζ) was identified as the key negative epigenomic regulator of dentin formation in odontoblasts.[15] However, the whole-genome epigenomic status changes of DPSCs during the pulp and dentin regeneration process remain unclear. To elucidate some of the underlying epigenomic mechanisms that contribute to dental pulp tissue regeneration and homeostasis, we recently reported an integrative epigenomic and transcriptome analysis of DPSCs during odontogenic differentiation to investigate how epigenetic status regulates gene expression changes.[16] Differentiating DPSCs exhibit a substantial increase in the number of super-enhancers, a local genomic location for condensed open chromatin peaks that facilitates transcriptional activities.

MS-275 and Trichostatin A (TSA) induce osteogenic differentiation *in vitro* and *in vivo*.[17—19] Short-term treatment with MS-275 induces the expression of odontogenic differentiation markers, such as *Runx2* and *DMP-1*, in DPSCs.[20] However, it remains unclear whether MS-275 and TSA exert beneficial effects on the odontogenic differentiation in DPSCs and subsequent matrix mineralization by differentiated DPSCs.

In this study, we explored the beneficial effects of MS-275 and TSA and their underlying mechanisms by conducting the Assay for Transposase-Accessible Chromatin using high-throughput sequencing (ATAC-seq), RNA-seq analyses, and *in vitro* assessment of odontogenic differentiation and maturation of DPSCs stimulated with MS-275 and TSA.

Materials and methods

Reagents

MS-275 (#S1053) was purchased from Selleck Chemicals (Houston, TX, USA). Trichostatin A (TSA) (#203-17561) was purchased from Fujifilm Wako Pure Chemical Corporation, Ltd. (Osaka, Japan).

Cell culture

Human DPSCs were purchased from Lonza, Inc. (Walkersville, MD, USA). DPSCs were cultured in low-glucose Dulbecco's modified Eagle's medium (DMEM; Thermo Fisher Scientific, Carlsbad, CA) supplemented with 100 units/mL of penicillin, 100 μg/mL of streptomycin, and 10 % fetal bovine serum (FBS; Biosera, Kansas City, MO). DPSCs were cultivated at 37 °C under humidified atmospheric conditions (5 % CO_2 and 95 % air). For inducing odontogenic differentiation, DPSCs were cultured in an induction medium (low-glucose DMEM with 10 % FBS, ascorbic acid (100 μg/mL), β-glycerophosphate (10 mM), and dexamethasone (10 nM)) for 30 days.

Alkaline phosphatase activity

Alkaline phosphatase (ALP) activity was measured as previously described.[21] It was normalized to cell numbers obtained from parallel cell culture and quantified using the Cell Counting Kit-8 assay (Dojindo, Kumamoto, Japan).[22]

Alizarin Red S staining

DPSCs were washed twice with Dulbecco's Phosphate-Buffered Saline (DPBS) and fixed with 70 % ethanol for 10 min. Fixed cells were washed with dH2O and stained

with 1 % Alizarin Red S (pH 4.2) solution. Images from each stained well were converted to a black/white scale for quantification. The average intensity of the area containing the cells was measured using ImageJ software. Because black and white were defined as low and high, respectively, on the black/white scale, the measured value was subtracted from the average intensity of an empty well.

Immunoblotting

Immunodetection was conducted as previously described.[23] Briefly, reduced samples were loaded onto NuPAGE Bis-Tris (Thermo Fisher Scientific) gels in MOPS buffer, and separated proteins were transferred onto a polyvinylidene fluoride membrane for immunodetection using the anti-Fibronectin (15613-1-AP, 1:1000, Proteintech, Rosemont, IL, USA), anti-HSP90β (GTX101448: GeneTex Inc, 1:2000), and anti-GAPDH (GTX100118: GeneTex Inc., 1:6000) antibodies as the primary antibodies.

ATAC-seq and data analyses

Following 9-day odontogenic induction, DPSCs were fixed with formaldehyde in the presence or absence of MS-275 or TSA, and ATAC-seq was performed using the ATAC-Seq Kit (#53150 Active Motif, Carlsbad, CA, USA) following the manufacturer's protocol. Prepared libraries were sequenced using 150-bp paired-end reads on a NovaSeq instrument.[24] Reads were processed as follows: trimming with Trimmomatic,[25] removal of PCR duplicates using MarkDuplicates, annotation to a reference genome (hg38) using Bowtie2 version 2.5.1,[26] and duplication comparison using deepTools.[27] The identification of significantly enriched chromatin peak using HOMER[28] have been described previously.[16]

Poly-A selection, strand-specific RNA-seq, and data analyses

Purified total RNA was DNase-treated and used in RNA-seq analyses as described previously.[29] For processing of the RNA-seq data, adapter trimming was conducted using Trim Galore version 0.6.5 (http://www.bioinformatics.babraham.ac.uk/projects/trim_galore/) with default settings, followed by alignment to the reference genome (hg38) using HISAT2 version 2.2.1.[30] Transcript expression at the exons was quantified using the "analyzeRepeast.pl" command in HOMER with "-strand both" and "-count exons" for MS-275-treated DPSCs or TSA-treated DPSCs as the target and non-treated DPSCs as the background. The expression ratio of all transcripts was calculated by dividing the expression level in MS-275-treated DPSCs or TSA-treated DPSCs by non-treated DPSCs. Transcripts with a ratio greater than 2 were identified as upregulated genes, while those with a ratio less than 0.5 were identified as downregulated genes by MS-275 and TSA. The original raw data from the ATAC-seq and RNA-seq analyses were deposited to the National Center for Biotechnology Information Gene Expression Omnibus database with the accession number GSE244059.

Transient siRNA transfection

Control siRNA (negative control DsiRNA) and 3 separate siRNAs for human Fibronectin 1 (FN1) (hs.Ri.FN1.13.1, hs.Ri.FN1.13.3, and hs.Ri.FN1.13.4) were purchased from Integrated DNA Technologies (Coralville, IA, USA). siRNAs were forward-transfected into DPSCs at a final concentration of 10 nM using Lipofectamine RNAiMAX (Thermo Fisher Scientific) reagent and incubated for 24 h, as previously described. [31,32]

Quantitative PCR analysis

Total RNA purification, cDNA preparation, and quantitative PCR (qPCR) were conducted as described previously.[33,34] Human *HPRT* was used as an internal reference control. The PCR primer sequences for the target genes are listed in Table 1.

Statistical analysis

Statistical analyses were performed using a one-way analysis of variance, followed by Bonferroni's (Fig. 1), Dunnett's (Fig. 2), Tukey's (Fig. 5D) tests, and two-tailed unpaired Student's t-tests (Fig. 5A).

Results

Determining the optimal HDACis concentrations for long-term stimulation

First, to determine the less-cytotoxic concentrations of MS-275 and TSA for long-term culture, DPSCs were cultured with the various concentrations of MS-275 and TSA (0.01—10.0 μM) for 9 days and the cell numbers were counted (Fig. 1). MS-275 (5.0 and 10.0 μM) and TSA (0.5, 1.0, 5.0, and 10.0 μM) caused a drastic decrease in cell numbers from day 6 after the MS-275 treatment and day 3 after the TSA treatment. MS-275 (1.0 μM) and TSA (0.1 μM) caused a minor decrease, but the decrease was not significant compared to that in non-treated cells. Thus, the maximum concentrations of MS-275 and TSA for long-term culture of DPSCs without apparent cytotoxicity were set at 1.0 and 0.1 μM, respectively.

MS-275 induced the formation of calcified nodules in DPSCs

To investigate whether MS-275 and TSA influence odontogenic differentiation in DPSCs as assessed by ALP activity and matrix mineralization-inducing ability in differentiated DPSCs as assessed by calcium nodule formation, cells were cultured for an extended period in the presence of MS-275 (1.0 μM) and TSA (0.1 μM). ALP activity and calcified nodule formation were evaluated every 3 days. None of the HDACis increased ALP activity in DPSCs (Fig. 2A). In contrast, Alizarin Red S staining revealed that MS-275, but not TSA, significantly induced calcified nodule formation on days 24, 27, and 30 compared with the untreated control (Fig. 2B).

Table 1 Primer pairs used in this study.

Primer name	Species	Direction	Sequence
FN1	Human	forward reverse	TCCACAAGCGTCATGAAGAG CTCTGAATCCTGGCATTGGT
HPRT	Human	forward reverse	TGGCGTCGTGATTAGTGATG CGAGCAAGACGTTCAGTCCT

FN = Fibronectin 1, HPRT = Hypoxanthine Phosphoribosyltransferase 1.

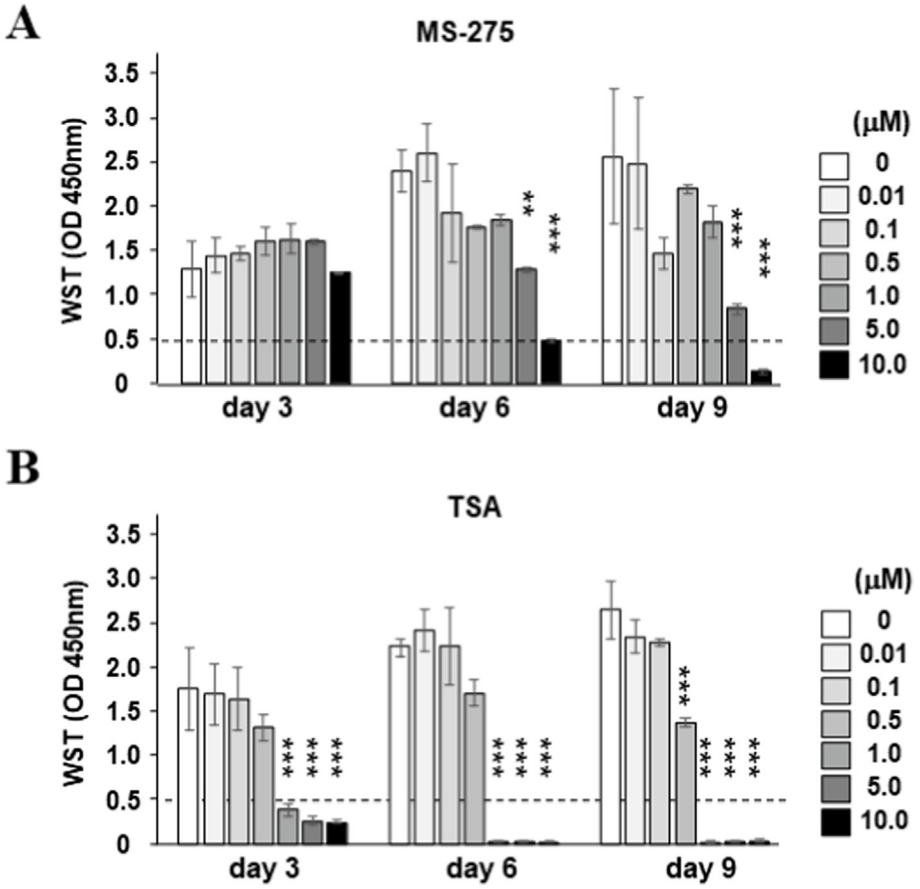

Fig. 1 Determining the optimal HDACi concentration for long-term stimulation DPSCs were cultured in an odontogenic induction medium for 9 days in the presence of various concentrations of MS-275 (A) or TSA (B). The number of cells was counted on days 3, 6, and 9. The average number of cells counted on day 0 is indicated by the dashed line. *$P < 0.05$; **$P < 0.01$; ***$P < 0.001$ significantly lower than non-treated DPSCs at each time point.

These results suggest that MS-275 induces calcified nodule formation without inducing odontogenic differentiation.

Subtle changes in open chromatin accessibility caused by MS-275 and TSA

Plot correlation analysis of ATAC-seq samples indicated complete concurrence of duplicate samples in untreated DPSCs, MS-275-treated DPSCs, and TSA-treated DPSCs (Spearman's R $>$ 0.98) (Fig. 3A). The correlations among the different experimental groups were also similar (Spearman's R $>$ 0.87). In particular, MS-275-treated DPSCs and TSA-treated DPSCs showed higher concurrence. Furthermore, principal component analysis (PCA) of ATAC-seq tags revealed only subtle changes in open chromatin accessibility peaks (OCAPs), as PC1 accounted for 97.5 % of the variance (Fig. 3B). Additionally, PCA of PC2 and PC3 indicated that MS-275-treated DPSCs and TSA-treated DPSCs were distinct from each other. ATAC-seq tags obtained on day 0 prior to the 9 days of odontogenic induction were precisely analyzed in accordance with a former study,[16] to validate the accuracy of the PCA. Integrated transcriptome and chromatin accessibility analyses revealed that higher ATAC-seq signals induced higher expression levels of the closest transcripts in MS-275-treated DPSCs and TSA-treated DPSCs (Fig. 3C). Previous reports of non-treated DPSCs showed comparable results.[16]

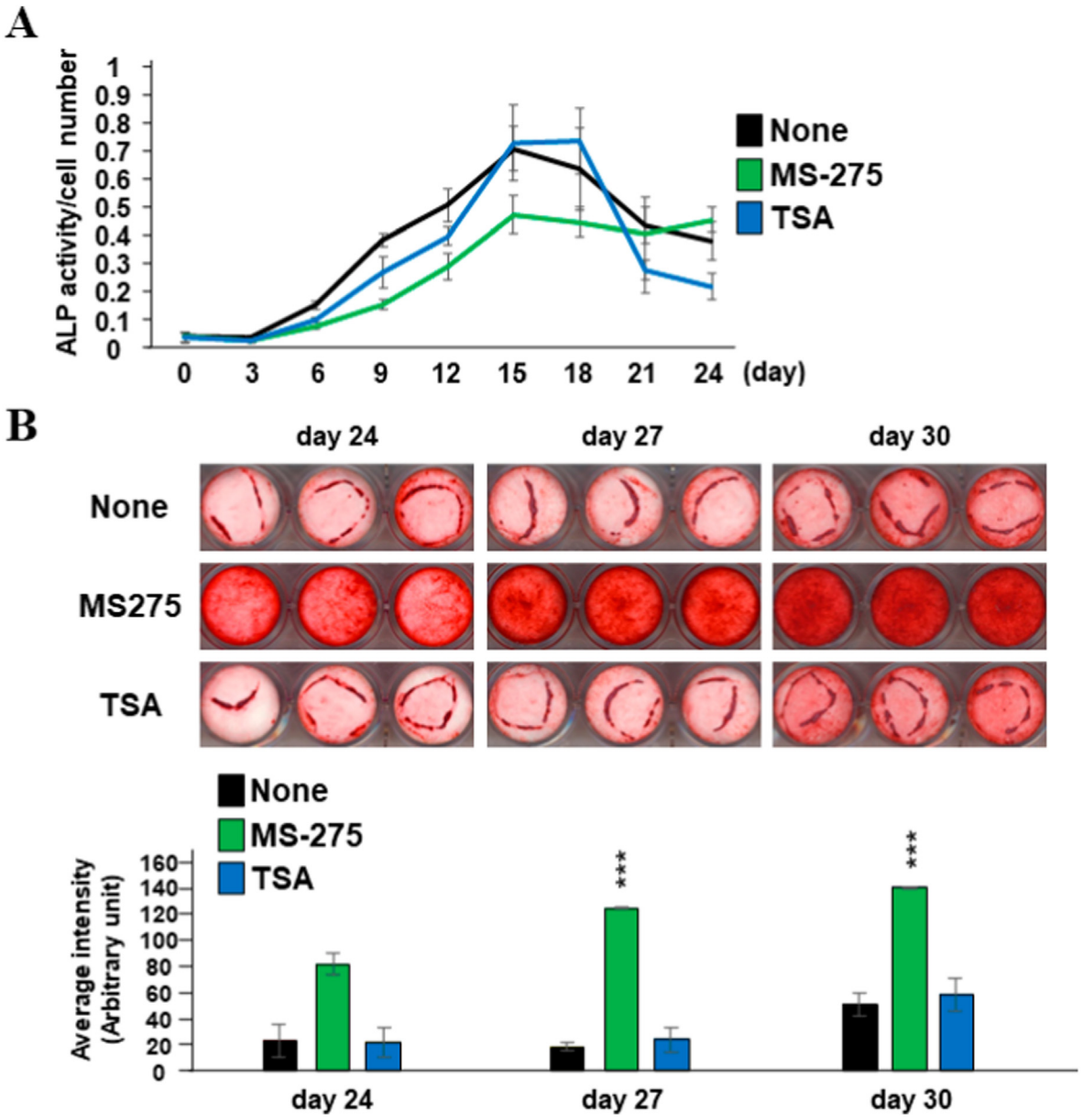

Fig. 2 MS-275 induced the formation of calcified nodules in DPSCs (A) DPSCs were cultured in an odontogenic induction medium for 24 days, and the ALP activity was evaluated. ALP activities were normalized using the Cell Counting Kit-8. (B) Alizarin Red S staining of DPSCs performed on days 24, 27, and 30. *$P < 0.05$; **$P < 0.01$; ***$P < 0.001$ significantly higher than non-treated DPSCs at each time point.

Comprehensive gene expression profiling identifies MS-275-induced up-regulation of extracellular matrix organization-related genes, unlike TSA

To comprehensively examine the gene expression changes induced by MS-275 or TSA treatment, DPSCs were cultured in an odontogenic induction medium for 9 days, and the RNA was collected. RNA-seq analyses of untreated and MS275-treated DPSCs showed that 2833 and 1928 transcripts (threshold = 2.0) were upregulated and downregulated, respectively, by the addition of MS-275 (Fig. 4A). However, only 14 and 1 transcripts (threshold = 2.0) were upregulated and downregulated, respectively, by TSA treatment (Fig. 4B).

The results of gene ontology analyses of the differentially expressed genes are shown in Fig. 4C. The upper rank of the pathway analyses of the enhanced biological processes in MS-275-treated DPSCs compared to non-treated DPSCs revealed that MS-275 treatment (red) specifically increased the expression of genes functionally related to the extracellular matrix (ECM), such as ECM organization and proteoglycans. Genes functionally related to the cell cycle were downregulated following MS-275 treatment (blue).

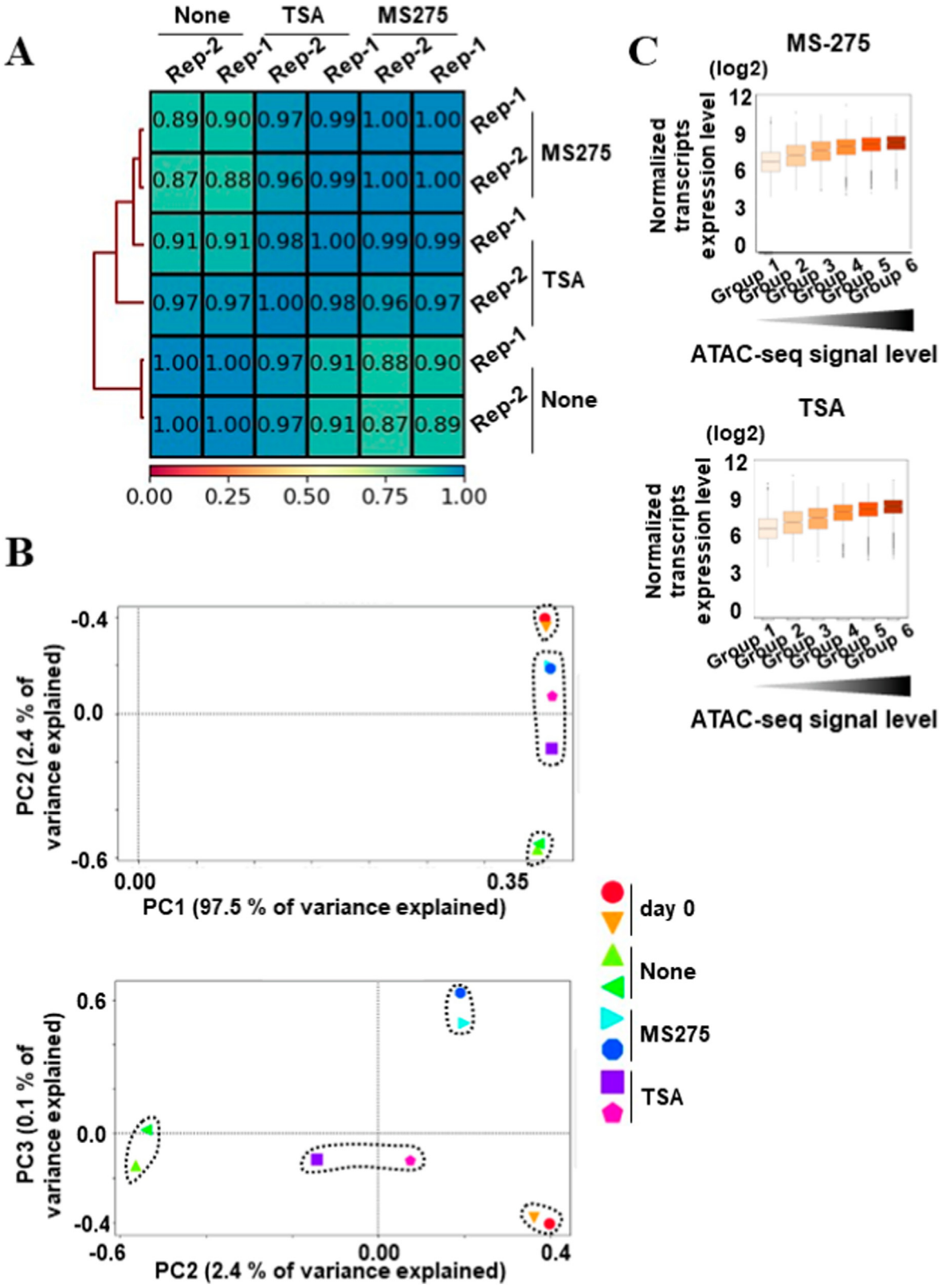

Fig. 3 Conservative open chromatin accessibility induced by treatment with MS-275 and TSA (A) Heatmaps of Spearman's correlation between two replicates of non-treated DPSCs, MS275-treated DPSCs, and TSA-treated DPSCs. (B) Principal component analysis. Upper dotplot using principal component (PC) 1 as the horizontal axis and PC2 as the vertical axis. Lower dotplot using PC2 as the horizontal axis and PC3 as the vertical axis. (C) Increased ATAC-seq signal level is correlated with the average expression level of the closest transcript of MS275-treated DPSCs and TSA-treated DPSCs.

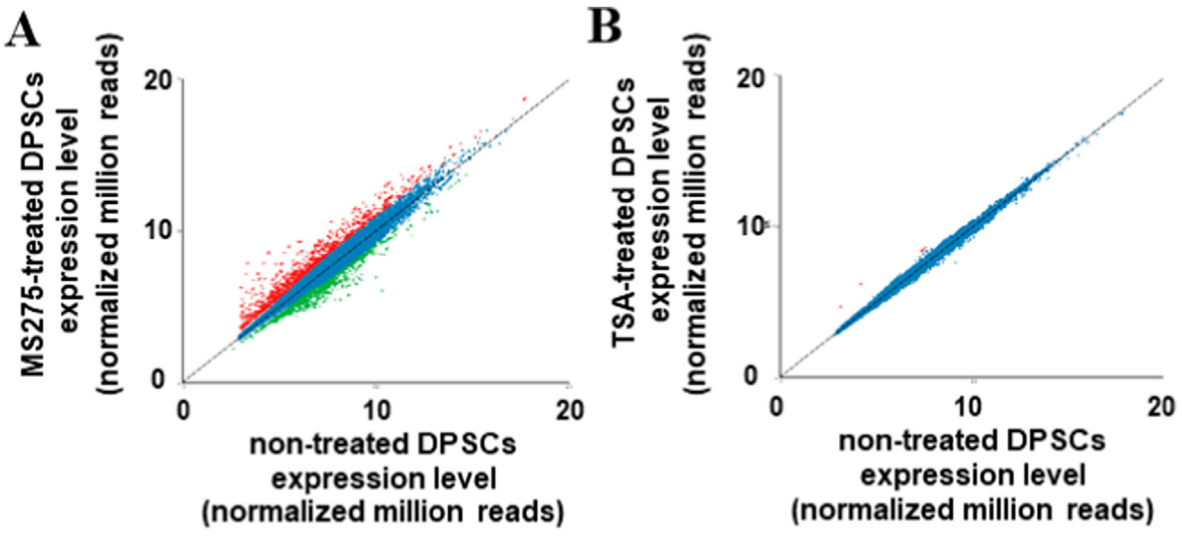

C

Up-regulated genes by MS275 treatment (933 genes)

Term	logP
Extracellular matrix organization	-17.8992
ECM proteoglycans	-11.4532
Integrin cell surface interactions	-11.4074
Non-integrin membrane-ECM interactions	-8.06934
Cell surface interactions at the vascular wall	-7.65019
Muscle contraction	-6.8216
Dissolution of fibrin clot	-6.6814
Neuronal system	-6.63738

Down-regulated genes by MS275 treatment (611 genes)

Term	logP
Cell cycle	-71.6662
Cell cycle, mitotic	-61.4466
Mitotic prometaphase	-51.2091
Resolution of sister chromatid cohesion	-48.1907
M phase	-34.1842
Mitotic metaphase and anaphase	-33.9658
RHO GTPases activate formins	-32.1582

Fig. 4 Comprehensive gene expression profiling reveals MS-275 induced up-regulation of extracellular matrix organization-related genes Whole-genome transcriptional changes assessed by RNA-seq. (A) Scatter plot comparing untreated DPSCs (x-axis) and MS-275-treated DPSCs (y-axis). (B) Scatter plot comparing untreated DPSCs (x-axis) and TSA-treated DPSCs (y-axis). (C) Gene Ontology analysis of genes upregulated and downregulated by MS-275 treatment. Red indicates terms associated with the extracellular matrix. Blue indicates terms associated with the cell cycle.

Fibronectin is required for MS-275-mediated calcium nodule formation

The ECM-related genes identified as MS-275-up-regulated genes (threshold = 2.0) were extracted (Table 2). Of these 30 genes, *FN1*, which encodes fibronectin, showed the highest expression. Consistently, a 9-day culture of DPSCs with MS-275 in odontogenic induction medium induced fibronectin expression (Fig. 5A). During the reparative dentin formation process, a fibronectin-positive irregular matrix was created.[35] Therefore, to assess the role of fibronectin in the increased calcium nodule formation induced by treatment with MS-275, fibronectin expression was knocked down using three independent siRNAs for *FN1*, and calcified nodule formation was evaluated. qPCR and SDS polyacrylamide gel electrophoresis analyses revealed successful suppression of fibronectin (Fig. 5B and C). Long-term odontogenic induction culture of siRNA-transfected DPSCs revealed that three kinds of siRNA for *FN1* were effective in suppressing MS-275-mediated increases in calcified nodule formation (Fig. 5D). These results indicated that fibronectin is indispensable for MS-275-mediated calcified nodule formation.

Discussion

In this study, we examined chromatin accessibility changes, transcriptome alterations, and odontogenic differentiation abilities of DPSCs through long-term treatment with two HDACis, including MS-275 and TSA. The results revealed that long-term stimulation with these HDACis was unable to modify whole-genomic chromatin accessibility (Fig. 3); however, MS-275 treatment specifically up-regulated ECM-coding genes (Fig. 4) and enhanced calcified nodule formation (Fig. 2B), possibly due to the up-regulation of fibronectin expression (Fig. 5), without affecting the odontogenic differentiation status of DPSCs (Fig. 2A).

Integrative epigenomic and transcriptome analyses of the untreated DPSCs and MS-275-treated DPSCs revealed that 2833 transcripts, including *FN1*, were upregulated by the addition of MS-275 (Fig. 4A) without apparent alteration of chromatin accessibility (Fig. 3). Two OCAPs enrichments in the intragenic and intergenic *FN1* gene loci were identified, and their enrichment depths remained unchanged by the addition of MS-275. This observation implies that expression changes in some transcripts, including *FN1*, are regulated by the binding of key transcription factors to the OCAPs, which triggers active gene transcription, rather than by the alteration in the degree of accessibility of adjacent OCAPs. Thus, a limitation of this study is the lack of a mechanistic explanation for the correlation between epigenomic and transcriptomic changes. Further studies, such as ChIP-seq and CUT&RUN-seq analyses, are required to fill this gap by exploring the whole-genome identification of the binding sites of key transcriptional factors, such as KLF4 and Osterix.[13,14]

MS-275, a specific inhibitor of HDAC1 and HDAC3, and TSA, a pan-HDAC inhibitor, were selected for this study because the positive effects of MS-275 and TSA on

Table 2 Relative expression levels obtained from normalized million reads of ECM-associated genes that were up-regulated by MS-275 treatment.

Annotation	None	MS-275
FN1	17.74	18.81
THBS1	15.17	16.22
SERPINE1	14.02	15.24
CTSB	13.91	14.47
ITGA5	12.51	12.80
PLOD1	11.11	11.74
SDC4	11.19	11.63
COL8A1	10.55	11.39
LTBP4	9.75	10.37
COL8A2	8.33	10.15
COL4A1	8.33	9.80
ITGA8	9.65	9.71
FMOD	8.74	9.60
TGFB2	11.43	9.59
NTN4	8.99	9.49
AGRN	9.19	9.46
NID2	8.70	9.34
ITGA4	8.80	8.87
ITGA7	7.96	8.78
ICAM1	6.89	8.25
DMD	7.56	8.31
MMP17	7.38	7.85
P3H2	6.34	6.47
PCOLCE2	6.00	6.43
ADAMTS10	4.58	5.34
LRP4	4.76	5.26
ICAM5	4.60	5.16
COL9A2	4.91	5.13
IBSP	2.74	2.87
BCAN	1.91	2.17

Comparable expression level between the genes and also between the treatments.
FN1 = Fibronectin 1, THBS1 = Thrombospondin 1, SERPINE1 = Serpin Family E Member 1, CTSB = Cathepsin B.
ITGA5 = Integrin Subunit Alpha 5, PLOD1 = Procollagen-Lysine,2-Oxoglutarate 5-Dioxygenase 1.
SDC4 = Syndecan 4, COL8A1 = Collagen Type VIII Alpha 1 Chain.
LTBP4 = Latent Transforming Growth Factor Beta Binding Protein 4, COL8A2 = Collagen Type VIII Alpha 2 Chain.
COL4A1 = Collagen Type IV Alpha 1 Chain, ITGA8 = Integrin Subunit Alpha 8, FMOD = Fibromodulin.
TGFB2 = Transforming Growth Factor Beta 2, NTN4 = Netrin 4, AGRN = Agrin, NID2 = Nidogen 2.
ITGA4 = Integrin Subunit Alpha 4, ITGA7 = Integrin Subunit Alpha 7, ICAM1 = Intercellular Adhesion Molecule 1.
DMD = Dystrophin, MMP17 = Matrix Metallopeptidase 17, P3H2 = Prolyl 3-Hydroxylase 2.
PCOLCE2 = Procollagen C-Endopeptidase Enhancer 2.
ADAMTS10 = ADAM Metallopeptidase With Thrombospondin Type 1 Motif 10.
LRP4 = LDL Receptor Related Protein 4, ICAM5 = Intercellular Adhesion Molecule 5.
COL9A2 = Collagen Type IX Alpha 2 Chain, IBSP = Integrin Binding Sialoprotein, BCAN = Brevican.

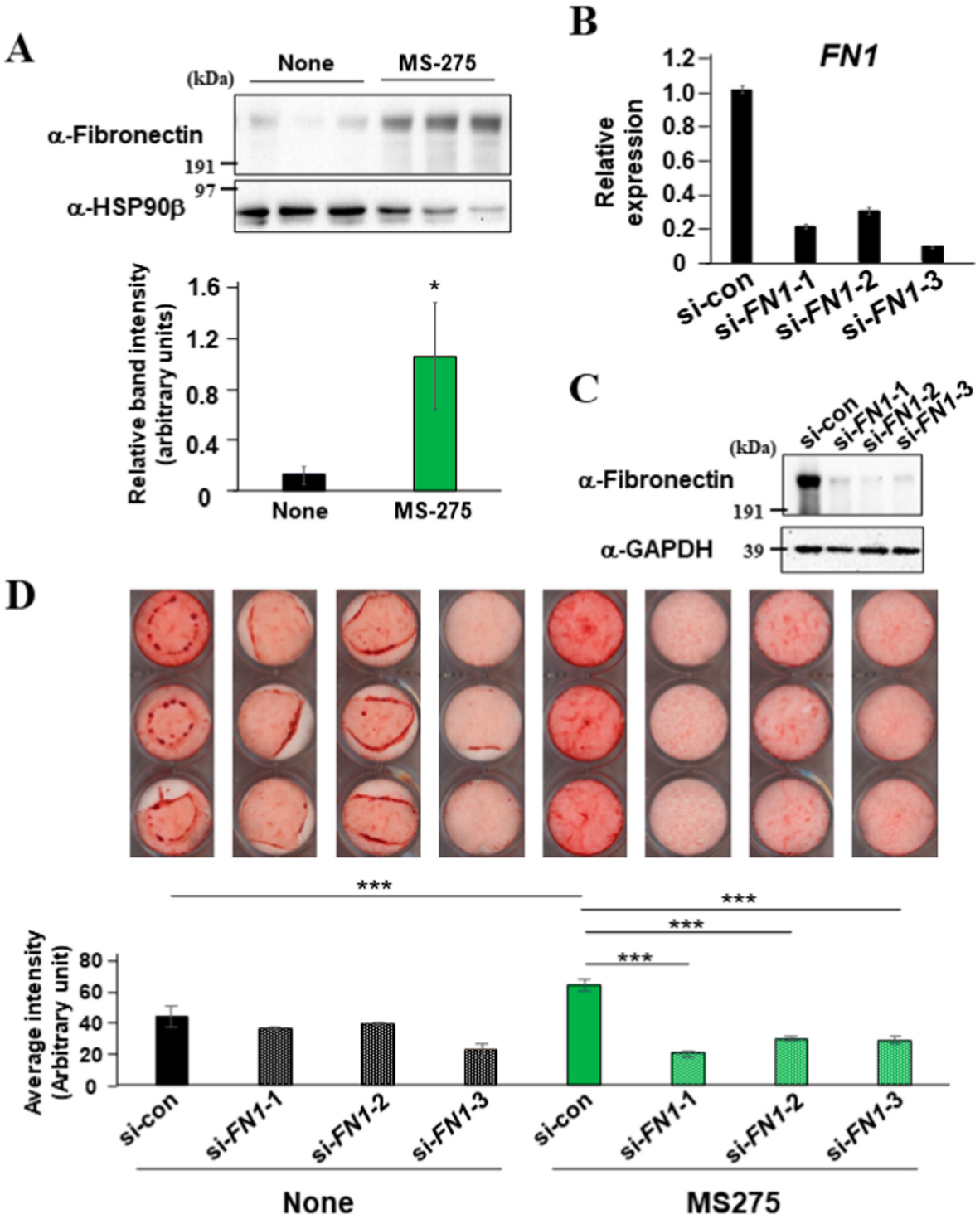

Fig. 5 Fibronectin is required for MS-275-mediated calcium nodule formation (A) DPSCs were stimulated with or without MS-275 (1.0 μM) in an odontogenic induction medium for 9 days. Whole cell lysate was collected, and FN1 expression was examined using specific antibodies. The membrane was also incubated with an HSP90β antibody as a loading control. (B) Three independent siRNAs for *FN1* were transfected into DPSCs for 24 h, and total RNA was collected to quantify the expression of *FN1*. *HPRT* was used for normalization. (C) DPSCs were transfected with either si-control or independent siRNAs for *FN1* for 24 h, and whole cell lysate was collected, and FN1 expression was examined using specific antibodies. The membrane was also incubated with a GAPDH antibody as a loading control. (D) DPSCs were transfected with si-control and three independent siRNAs for *FN1* (si-*FN1*-1, si-*FN1*-2, si-*FN1*-3) for 24 h, followed by stimulation with or without MS-275 (1.0 μM) in odontogenic induction medium for 24 days. Alizarin Red S staining was performed on day 24. si-con = si-control $^{*}P < 0.05$; $^{**}P < 0.01$; $^{***}P < 0.001$ significantly different.

osteogenesis are widely known.[17–19] Similar to TSA and MS-275, DPSCs were treated with RGFP966, an inhibitor of HDAC3, for 9 days. Whole epigenomic changes were nominal and equivalent to TSA and MS-275 (data not shown). Therefore, the relationship between HDAC inhibitor-induced DPSC phenotypes and the inhibitory abilities of HDAC inhibitors should be carefully assessed.

Fibronectin was identified as a key molecule in MS-275-induced calcified nodule formation in differentiated DPSCs. During the reparative dentin formation process, by direct pulp capping with $Ca(OH)_2$, a fibronectin-positive irregular matrix was created, and an odontoblast-like cell layer was located directly beneath it.[35] This *in vivo* finding suggested the prominent role of fibronectin in calcified nodule formation by pulp residential cells such as DPSCs. In addition, fibronectin is a multi-functional protein that can bind to collagen, induce cellular functions through its RGD (Arg-Gly-Asp) domain-integrin receptor interaction, and efficiently trap growth factors extracellularly, releasing them in a temporo-spatial manner.[36,37] Since the efficiency of siRNA does not last for long in DPSCs,[38] suppressing calcified nodule formation using siRNAs for *FN1* implies that fibronectin is required in the early stages of the construction of an organized ECM microenvironment during odontogenic differentiation. Approximately 12 % of the cells in dental pulp tissues are considered to be DPSCs[5,39]; therefore, DPSCs are not the only cell population to contribute to pulp tissue regeneration. Further studies are necessary to evaluate the potential of MS-275 for cells with matrix mineralization-inducing abilities in pulp tissue.

In conclusion, among the HDACis examined in this study, MS-275 induced calcified nodule formation through the upregulation of fibronectin without apparent epigenomic changes in DPSCs. Therefore, MS-275, a direct capping material, has therapeutic potential for DPSC-induced reparative dentin formation in a fibronectin-organizing physiological ECM environment that is adequate for matrix mineralization.

Declaration of competing interest

The authors have no conflicts of interests to declare.

Acknowledgments

This study was financially supported by JSPS KAKENHI grant numbers 22H03266 and 22K19611 for Shigeki Suzuki, and 20H03862, 20K21668, and 23K18350 for Satoru Yamada.

Appendix A. Supplementary data

Supplementary data to this article can be found online at https://doi.org/10.1016/j.jds.2023.11.019.

References

1. Allis CD, Jenuwein T. The molecular hallmarks of epigenetic control. *Nat Rev Genet* 2016;17:487–500.
2. Kouzarides T, Bannister AJ. Regulation of chromatin by histone modifications. *Cell Res* 2011;21:381–95.
3. Suzuki S, Yamada S. Epigenetics in susceptibility, progression, and diagnosis of periodontitis. *Jpn Dent Sci Rev* 2022;58:183–92.
4. Kim HI, Bae SC. Histone deacetylase inhibitors: molecular mechanisms of action and clinical trials as anti-cancer drugs. *Am J Transl Res* 2011;3:166–79.
5. Masuda K, Han X, Kato H, et al. Dental pulp-derived mesenchymal stem cells for modeling genetic disorders. *Int J Mol Sci* 2021;22:2269.
6. Heo SC, Keum BR, Seo EJ, et al. Lysophosphatidic acid induces proliferation and osteogenic differentiation of human dental pulp stem cell through lysophosphatidic acid receptor 3/extracellular signal-regulated kinase signaling axis. *J Dent Sci* 2023;18:1219–26.
7. Kim Y, Park HJ, Kim M-K, et al. Naringenin stimulates osteogenic/odontogenic differentiation and migration of human dental pulp stem cells. *J Dent Sci* 2023;18:577–85.
8. Jin C, Zhao S, Xie H. Forskolin enhanced the osteogenic differentiation of human dental pulp stem cells in vitro and in vivo. *J Dent Sci* 2023;18:120–8.
9. Zhou D, Gan L, Peng Y, et al. Epigenetic regulation of dental pulp stem cell fate. *Stem Cell Int* 2020;2020:8876265.
10. Suzuki S, Sreenath T, Haruyama N, et al. Dentin sialoprotein and dentin phosphoprotein have distinct roles in dentin mineralization. *Matrix Biol* 2009;28:221–9.
11. Suzuki S, Haruyama N, Nishimura F, Kulkarni AB. Dentin sialophosphoprotein and dentin matrix protein-1: two highly phosphorylated proteins in mineralized tissues. *Arch Oral Biol* 2012;57:1165–75.
12. Liu HJ, Wang T, Li QM, Guan XY, Xu Q. Knock-down of p300 decreases the proliferation and odontogenic differentiation potentiality of HDPCs. *Int Endod J* 2015;48:976–85.
13. Wang T, Liu H, Ning Y, Xu Q. The histone acetyltransferase p300 regulates the expression of pluripotency factors and odontogenic differentiation of human dental pulp cells. *PLoS One* 2014;9:e102117.
14. Tao H, Lin H, Sun Z, et al. Klf4 promotes dentinogenesis and odontoblastic differentiation via modulation of TGF-β signaling pathway and interaction with histone acetylation. *J Bone Miner Res* 2019;34:1502–16.
15. Yuan H, Suzuki S, Terui H, et al. Loss of IκBζ drives dentin formation via altered H3K4me3 status. *J Dent Res* 2022;101:951–61.
16. Sasaki K, Suzuki S, Fahreza RR, Nemoto E, Yamada S. Dynamic changes in chromatin accessibility during the differentiation of dental pulp stem cells reveal that induction of odontogenic gene expression is linked with specific enhancer construction. *J Dent Sci* 2023 (in press).
17. Kim HN, Lee JH, Bae SC, et al. Histone deacetylase inhibitor MS-275 stimulates bone formation in part by enhancing Dhx36-mediated TNAP transcription. *J Bone Miner Res* 2011;26:2161–73.
18. Bae HS, Yoon WJ, Cho YD, et al. An HDAC inhibitor Entinostat/MS-275, partially prevents delayed cranial suture closure in heterozygous Runx2 null mice. *J Bone Miner Res* 2017;32:951–61.
19. Lawlor L, Yang XB. Harnessing the HDAC-histone deacetylase enzymes, inhibitors and how these can be utilised in tissue engineering. *Int J Oral Sci* 2019;11:20.
20. Lee EC, Kim YM, Lim HM, Ki GE, Seo YK. The histone deacetylase inhibitor (MS-275) promotes differentiation of human dental pulp stem cells into odontoblast-like cells independent of the MAPK signaling system. *Int J Mol Sci* 2020;21:5771.
21. Hirata-Tsuchiya S, Suzuki S, Okamoto K, et al. A small nuclear acidic protein (MTI-II, Zn2+-binding protein, parathymosin) attenuates TNF-α inhibition of BMP-induced osteogenesis by

enhancing accessibility of the Smad4-NF-κB p65 complex to Smad binding element. *Mol Cell Biochem* 2020;469:133—42.
22. Yoshida K, Suzuki S, Kawada-Matsuo M, et al. Heparin-LL37 complexes are less cytotoxic for human dental pulp cells and have undiminished antimicrobial and LPS-neutralizing abilities. *Int Endod J* 2019;52:1327—43.
23. Jaha H, Husein D, Ohyama Y, et al. N-terminal dentin sialoprotein fragment induces type I collagen production and upregulates dentinogenesis marker expression in osteoblasts. *Biochem Biophys Rep* 2016;6:190—6.
24. Bai J, Lin Y, Zhang J, et al. Profiling of chromatin accessibility in pigs across multiple tissues and developmental stages. *Int J Mol Sci* 2023;24:11076.
25. Bolger AM, Lohse M, Usadel B. Trimmomatic: a flexible trimmer for Illumina sequence data. *Bioinformatics* 2014;30:2114—20.
26. Langmead B, Salzberg SL. Fast gapped-read alignment with Bowtie 2. *Nat Methods* 2012;9:357—9.
27. Ramírez F, Dündar F, Diehl S, Grüning BA, Manke T. deepTools: a flexible platform for exploring deep-sequencing data. *Nucleic Acids Res* 2014;42:W187—91.
28. Heinz S, Benner C, Spann N, et al. Simple combinations of lineage-determining transcription factors prime cis-regulatory elements required for macrophage and B cell identities. *Mol Cell* 2010;38:576—89.
29. Yuan H, Suzuki S, Hirata-Tsuchiya S, et al. PPARγ-induced global H3K27 acetylation maintains osteo/cementogenic abilities of periodontal ligament fibroblasts. *Int J Mol Sci* 2021;22:8646.
30. Kim D, Langmead B, Salzberg SL. HISAT: a fast spliced aligner with low memory requirements. *Nat Methods* 2015;12:357—60.
31. Suzuki S, Hoshino H, Yoshida K, et al. Genome-wide identification of chromatin-enriched RNA reveals that unspliced dentin matrix protein-1 mRNA regulates cell proliferation in squamous cell carcinoma. *Biochem Biophys Res Commun* 2018; 495:2303—9.
32. Suzuki S, Yuan H, Hirata-Tsuchiya S, et al. DMP-1 promoter-associated antisense strand non-coding RNA, panRNA-DMP-1, physically associates with EGFR to repress EGF-induced squamous cell carcinoma migration. *Mol Cell Biochem* 2021;476: 1673—90.
33. Suzuki S, Fukuda T, Nagayasu S, et al. Dental pulp cell-derived powerful inducer of TNF-α comprises PKR containing stress granule rich microvesicles. *Sci Rep* 2019;9:3825.
34. Yamamoto T, Yuan H, Suzuki S, Nemoto E, Saito M, Yamada S. Procyanidin B2 enhances anti-inflammatory responses of periodontal ligament cells by inhibiting the dominant negative pro-inflammatory isoforms of peroxisome proliferator-activated receptor. *J Dent Sci* 2023 (in press).
35. Yoshiba K, Yoshiba N, Nakamura H, Iwaku M, Ozawa H. Immunolocalization of fibronectin during reparative dentinogenesis in human teeth after pulp capping with calcium hydroxide. *J Dent Res* 1996;75:1590—7.
36. Suzuki S, Kobuke S, Haruyama N, Hoshino H, Kulkarni AB, Nishimura F. Adhesive and migratory effects of phosphophoryn are modulated by flanking peptides of the integrin binding motif. *PLoS One* 2014;9:e112490.
37. Dalton CJ, Lemmon CA. Fibronectin: molecular structure, fibrillar structure and mechanochemical signaling. *Cells* 2021;10:2443.
38. Yoshida K, Suzuki S, Yuan H, et al. Public RNA-seq data-based identification and functional analyses reveal that MXRA5 retains proliferative and migratory abilities of dental pulp stem cells. *Sci Rep* 2023;13:15574.
39. Pagella P, de Vargas Roditi L, Stadlinger B, Moor AE, Mitsiadis TA. A single-cell atlas of human teeth. *iScience* 2021; 24:102405.